2010 IEEE International Conference on Robotics and Automation
Anchorage Convention District
May 3-8, 2010, Anchorage, Alaska, USA

Real-Time Remote Transmission of Multiple Tactile Properties through Master-Slave Robot System

Takahiro Yamauchi, Shogo Okamoto, Masashi Konyo, Yusuke Hidaka, Takashi Maeno, and Satoshi Tadokoro

Abstract— **Remote transmission of high quality sense of touch requires the representation of multiple tactile properties and compensation of communication delay. We developed a real-time remote transmission system that can deliver multiple tactile properties using a master-slave robot system. First, we assessed what type of tactile properties should be transmitted and how to connect them in real time. Three tactile properties—roughness, friction, and softness—were transmitted on the basis of the real-time estimated physical properties of three main wavelengths, a kinetic friction coefficient, and spring constants, respectively. Tactile stimulations were generated in synchronization with hand exploration at the master side by using local tactile generation models to compensate for communication time delay. The transmission of multiple tactile properties was achieved by the integration and enhancement of our previously reported methods for vibrotactile displays and tactile sensors. A discrimination experiment using different materials showed the feasibility of the total system involving the three tactile properties.**

I. Introduction

Cutaneous sensation is required in a number of applications such as a robotic surgery system and dexterous telemanipulation system to transmit more realistic contact information from a remote site. One important issue, however, is that cutaneous sensation requires the representation of multiple tactile properties because these are based on multiple physical properties. For example, tactile information is expressed using multiple adjectives such as rough/smooth, soft/hard, sticky/slippery, and warm/cool. Another issue is the asynchronous transmission between hand exploration and tactile feedback due to communication delay. Human tactile perception is closely related to hand exploration. The decoupled relation between them adversely affects tactile sensation. For example, the authors confirmed that a delay of approximately 40 ms in tactile feedback in response to hand movement caused changes in tactile sensation [1]. To solve these problems, we present a feasibility study of a real-time remote transmission system for multiple tactile properties.

Several studies have reported remote tactile transmission systems that deliver tactile information detected by a remote tactile sensor to the operator. For example, tactile transmission systems for a medical gripper or glove used in minimally invasive surgery or palpation were reported [2] [3]. These studies aim to transmit pressure distribution and total load in the contact area between the probe and body tissue. A tactile transmission system for a prosthetic leg, which transferred the position of center of gravity and total load in the sole, was also developed [4]. A prosthetic hand that transferred pressure in the hand to the user was also developed [5]. Several master-slave-type robot systems aim to transfer tactile information, such as pressure [6] and high-frequency vibrations [7] [8], from the slave hand to the master side to support telemanipulation. Yamamoto et al. developed a master-slave system that transfers vibration detected by a tactile sensor running on material surfaces for the transmission of texture information [9]. The above-mentioned studies basically focused on a special use and a particular tactile property. On the other hand, Caldwell et al. [10] reported a transmission system for multiple tactile properties. Their system delivered roughness on a textured surface, vibration delivered from stick-slip friction, total load, and temperature change to the operator. However, they did not demand natural tactile sensation for the operator because the total load was symbolically replaced by a stepwise vibration intensity. In addition, no studies have dealt with the compensation of communication delay to synchronize tactile stimulation with hand exploration.

The authors of this study have proposed tactile display methods using vibratory stimulation for representing roughness, softness [11], and friction [12]. These methods were based on frequency response characteristics of human mechanoreceptors. It is expected that the superposition of these vibratory stimulations can represent multiple tactile properties simultaneously. We have partly confirmed that such superposition could represent several tactile feelings such as those of cloth materials [11], in which the tactile display methods for each tactile property are not well connected to the physical properties of the materials. In addition, the authors have also developed a tactile sensor that can estimate multiple physical factors, including wavelength of textured surfaces, friction coefficients, and Young's modulus, which are related to the tactile properties [13].

In this paper, we report the first trial of an integration of our tactile sensor and display systems. We develop a remote transmission for multiple tactile properties through a master-slave robot system in real time. It is a key component for the integration how to transmit the signals detected by the tactile sensor to the tactile display. We discuss what type of tactile properties should be transmitted and how to connect them in real time. Real-time synchronization between master and slave sides is a critical issue for tactile transmission, as mentioned above. We apply a time-delay compensation method, which has been proposed in a previous study [14]. In this method, tactile stimulation can be generated in

T. Yamauchi, S. Okamoto, M. Konyo, and S. Tadokoro are with the Graduate School of Information Sciences, Tohoku University, 6-6-1, Aramaki Aza Aoba, Aoba-ku, Sendai, Miyagi, 980-8579, Japan. {konyo, tadokoro}@rm.is.tohoku.ac.jp

Y. Hidaka and T. Maeno are with the Graduate School of System Design and Management, Keio University, 4-1-1 Hiyoshi, Kohoku-ku, Yokohama, Kanagawa, 223-8522, Japan

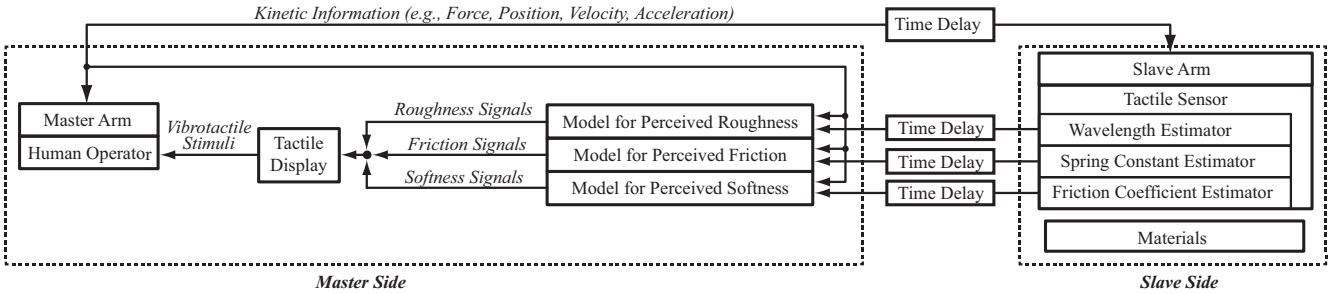

Fig. 1. Block Diagram of Master-Slave-Type Tactile Transmission System for Multiple Tactile Properties

synchronization with hand exploration at the master side by using a local tactile generation model. This paper is the first report that applies the concept to multiple tactile properties. To develop the transmission system, we enhance the tactile sensing methods developed by the authors [13] to achieve more detailed properties robustly in real time. We combine physical parameters estimated by the tactile sensor with the tactile displayed methods developed by the authors [11] [12] with several improvements. Finally, we confirm the feasibility of the total system involving three tactile properties selected through a material discrimination test.

II. System Design

A. Selection of Multiple Tactile Properties

In general, haptic cues for object recognition are categorized into material properties and geometric properties [17].

Geometric properties represent volume or shape of the object. This information can be provided by a force-feedback device. This paper does not focus on force-feedback methods because many studies have been proposed for time-delay communication [15] [16]. On the other hand, material properties are highly related to tactile properties. We, however, do not have the generalized classification for tactile properties. Different classifications of tactile properties have been reported mainly because the classifications depend on the target material. For example, roughness, softness, and temperature are clearly used in recognition of material [17]. Hollins et al. reported that roughness, softness, and sticky/slippery are perceptual bases [18]. Yoshioka et al. determined that these three factors explain 96%–97% of the perceived variances of textures and that information on stickiness has a high correlation coefficient between kinetic friction coefficients of textures [19]. According to Shirado et al., dry/wet is considered to be another possible tactile property in addition to roughness and softness [20]. Note that friction coefficients are related to both sticky/slippery and dry/wet sensations [21]. On the other hand, Shirado et al. reported that friction coefficients are not attributed to an independent tactile property because they affect several tactile properties in a cross-sectoral manner [20].

In this study, we selected three tactile properties—roughness, softness, and friction—which have reasonable agreement with conventional classification. Furthermore, these properties have been used in our tactile display and sensing methods. We attempted to combine both methods in real-time transmission and to verify the tactile transmission quality by testing discrimination scores of several materials to confirm the feasibility of the combinations.

B. Synchronization of Hand Exploration and Tactile Feedbacks

In order to cancel the temporal gap between the operator's manipulation and corresponding sensory feedback, a local model of the remote environment, such as geometric information, is constructed at the master-side system [15]. In the case of tactile feedback, the local model includes physical parameters of textures that affect tactile sensations. For instance, a tactile-roughness transmission system constructs a local model involving the surface wavelengths of textures [14].

In this study, we applied this method for friction and softness transmission in addition to roughness. We assumed that the physical parameters of friction and softness properties are friction coefficients and spring constants, respectively. Fig. 1 shows a block diagram of the developed system. This system has a standard force-reflecting-type force feedback for kinetic information. In addition, the tactile sensor installed on the slave-side system estimates physical parameters of target materials in real time. The estimated physical parameters are transferred to the local models of the master-side system. The local models continue to be updated by the transferred physical parameters. In the master-side system, tactile stimuli are generated by combining the hand movements of the operator and local models. Since the tactile stimuli and hand movements are synchronized, there is no temporal gap between the tactile feedback and the operator's movements.

This method does not compensate for the delay of physical parameters itself because it is affected by the estimation time at the slave side and communication delay. If the remote material changes rapidly, the tactile feedback cannot follow the change of materials. However, the change of material usually corresponds to movement of the operator's hand, which is not conducted at more than several Hz. As described later, our update rates of physical parameters are enough high compared to hand movements (250 Hz for wavelengths and friction coefficients and 125 Hz for spring constants).

C. Transmission between Measured and Displayed Signals

An important aspect of transmission is how to connect measured signals at the tactile sensor with stimulations at the tactile display. As we mentioned in Section II-B, measured signals should be converted into physical parameters at the

slave side to apply our compensation method for communication delay. Thus, the tactile display methods should be related to the physical parameters. We considered the connection of signals by dividing into each tactile property as follows.

For the roughness property, we have confirmed that vibrotactile stimulation based on surface wavelengths and hand speed can represent the roughness sensation [14] (Section IV-B and Section V-A).

For the friction property, the human perception mechanism of friction is not well understood. We have suggested that high-frequency vibrations on the finger skin generated by stick-slip phenomena can be a cue for understanding the friction property [12]. We proposed a friction display method that reproduces approximate stick-slip transition based on a model of a single-DOF vibration system with Coulomb friction. If the tactile sensor at the slave side could measure the human-like stick-slip phenomena, the physical parameters in the approximate model should be transmitted to the master side. However, it is very difficult to reproduce stick-slip phenomena in the same manner as human skin because the tactile sensor has different friction characteristics. In this study, we selected friction coefficients measured by a three-axis force sensor as physical parameters (Section IV-C). At the master side, the friction display model generates stick-slip transition based on measured friction coefficients and fixed material parameters, which were determined by observations of contact between human skin and an acrylic plate in a previous study [12] (Section V-B). In this sense, the friction display in this study does not reflect real material properties. However, we have confirmed that changes of friction coefficients can control the magnitude of perceived friction sensation [12]. This means that the measured friction coefficients can represent the magnitude of friction sensation even using fixed material properties.

For the softness property, the human perception mechanism of softness is less understood. In this study, we assumed that a spring constant represents the physical parameter of stiffness, which is related to the softness property. Note that Young's Modulus, which was used in [13], does not reflect the stiffness related to the geometric shape of a material; the spring constant is better as a measure of stiffness. We propose a real-time estimation method of spring constants at the slave side (Section IV-D). For the display, we assumed that the amount of activity of the SA I-type mechanoreceptor is related to the softness property. This assumption can be supported by results of a previous study that perceived softness can be controlled by changing the contact area against the pushing force [22] because human detection of the contact area is highly related to the activity of SA I. To control the activity of SA I at the master side, we used the pressure display method that we proposed previously [11]. This method produces a static pressure sensation using vibrotactile stimuli at a very low frequency (< 5 Hz) where SA I is more sensitive than other mechanoreceptors. Thus, the activity of SA I can be controlled by the amplitude of the low-frequency vibrations. However, this method cannot be immediately applied to the tactile transmission system. This is because the relationship between the estimated spring constant and the vibration amplitude is not clear. In the present study, we assumed a simple inversely proportional relationship between the spring constants and the displayed amplitudes (Section V-C). These relationships need to be elucidated in the future.

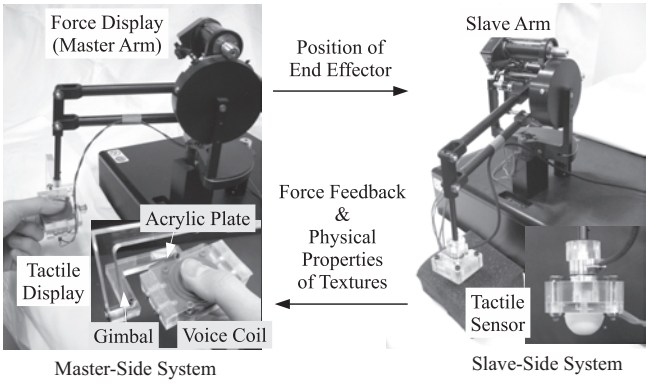

Fig. 2. Schematic View of Master-Slave System

III. Development of Master-Slave System

We first provide an overview of the master-slave system. Fig. 2 shows the developed master-slave system. For robot arms, PHANToM Premiums (SensAble Technologies) were adopted. The force feedback was conducted as a force-reflecting type based on a force sensor attached to the slave arm. A human mimetic tactile sensor, which is described in Section IV-A, was installed on the slave arm. A tactile display, which was installed on the master arm, is required to generate single-DOF vibrations against finger skin in the vertical direction with enough force. We have confirmed that even single-DOF vibrations can represent multiple tactile sensations (pressure sensation, roughness sensation, and friction sensation) by selecting vibration frequency and controlling vibration amplitude in response to hand movement [11]. In this study, a voice coil type speaker (AURA, SOUND/NSW1-205-8A) was used for the vibrator. The speaker corn was covered by a 0.5-mm thick acrylic plate. Stimulation of finger skin was provided through the vibration of this plate. The vibrator was connected to the robot arm with a gimbal mechanism, which allowed operators to smoothly move their hands.

The detailed sensing methods and display methods for each tactile property are described in Sections IV and V, respectively.

IV. Tactile Sensor and Sensing Methods

A. Tactile Sensor

A tactile sensor for the tactile transmission system was required for estimating surface wavelengths, friction coefficients, and spring constants, as described in Section II. A tactile sensor that the authors developed [13] satisfies these requirements. The sensor adopted in this study is a hemispherical version [23] of this tactile sensor, such that the sensor is able to scan the texture in its planar direction.

Fig. 3 shows the tactile sensor used in this study. The sensor is composed of a hemispherical silicone rubber and

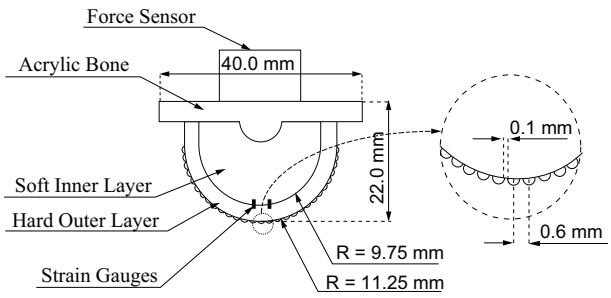

Fig. 3. Schematic View of Tactile Sensor

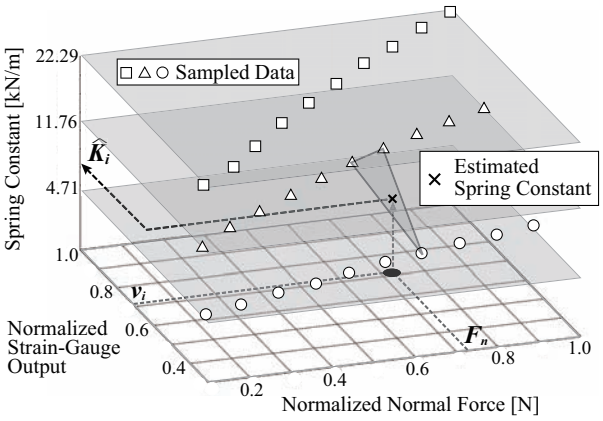

Fig. 4. Mapping Model for Estimating Spring Constants

a force sensor (NITTA, EFS-18M20A25-M10). The hemispherical rubber is formed as a hard outer layer and a soft inner layer. The outer layer is covered with distal ridges with widths of 0.5 mm and intervals of 0.6 mm close to that of the epidermal ridges of a human finger. As transducers, four strain gauges are embedded at the border of two layers just beneath the distal ridges. The disposition of the gauges was designed such that the gauges efficiently respond to the vibration of the ridges [13]. The strain gauges are connected to the control computer by way of a strain amplifier. The strain signals are sampled at 5 kHz.

B. Estimation of Surface Wavelengths

The estimation method for the surface wavelength of textures is the same as the Fast Fourier Transformation (FFT) based method we used previously [14]. Because of the surface roughness of the textures, the sensor vibrates when scanning the textures. The strain gauges respond to this vibration. By computing the FFT of the output voltages of the strain gauges, the vibratory frequency of the sensor is acquired. The surface wavelength of the texture is determined by $\lambda = |v(t)|/f(t)$, where λ, $v(t)$, and $f(t)$ are the surface wavelength, scanning velocity of the sensor, and vibratory frequency of the sensor, respectively.

In order to estimate the vibratory frequencies of the sensor, the computed power spectrum is used. N peaks are extracted from the power spectrum. The frequencies corresponding to each peak are f_1, f_2..., f_N, and the corresponding powers are A_1, A_2..., A_N, where $A_1 > A_2 ... > A_N$, which means the power peaks are extracted in descending order. A_i is used for determining the amplitude of the roughness stimuli in Section V-A. We confirmed that this sensor could detect at least 0.2 mm wavelength when the velocity was 20 mm/s and the normal force was 1.0 N. The estimation accuracy decreases when the normal force is small and the hand movement is slow. Thus, the wavelengths and the powers were updated only when the normal force was more than 0.2 N and the hand velocity was more than 50 mm/s. The update rate was 250 Hz.

C. Estimation of Friction Coefficients

The stick-slip model for the friction display, as described in Section V-B, requires both kinetic and static friction coefficients. However, it is difficult to estimate the static friction coefficients because the developed tactile sensor has a small sticking phase when stroking with materials. In this study, we focused on transmitting the friction coefficients rather than the reproduction of accurate stick-slip phenomena, as described in Section II-C. Thus, we assumed that the perceived friction is related to the kinetic friction coefficient and the static friction coefficients are simply proportional to the kinetic coefficients.

Friction coefficients between the tactile sensor and materials were estimated using the force sensor. The friction coefficients were determined by

$$\mu_k = \frac{|F_t|}{|F_n|}, \tag{1}$$

$$\mu_s = 2\mu_k \tag{2}$$

where F_t and F_n are the lateral force and normal force exerted to the sensor. The force data were sampled at 1 kHz, and the estimated values were determined by the average for 20 ms. The estimation becomes unstable when the normal force is small and the hand exploration is in turn-round motion. Thus, the friction coefficients were updated only when the normal force was more than 0.2 N and the hand velocity was more than 40 mm/s. The update rate was 250 Hz.

D. Estimation of Spring Constants

When the tactile sensor is pressed into elastic objects, its deformation depends on the elasticity of the objects and the normal force applied to the sensor when the tactile sensor has a constant elasticity. The magnitude of the deformation reflects on the outputs of the strain gauges embedded in the sensor. The authors previously proposed a method to estimate the elasticity of target objects from the variance of the strain gauge outputs [13]. However, the variance was susceptible to manufacturing error in the arrangement of the strain gauges. In the present study, we adopt a more robust method, using a mapping table determined by a prior experiment as follows.

In order to prepare the mapping table for each strain gauge, the sensor was thrust into three silicone rubber samples with known spring constants (4.71, 11.76, 22.29 [kN/m]). These spring constants were calculated as a reduced value regarding

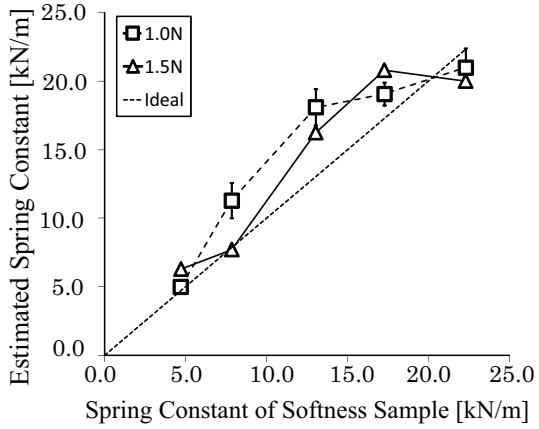

Fig. 5. Validation of Estimation Method for Spring Constants (Error bars for 1.5 N are too small to be seen)

the shape of the samples as a cylinder 20 mm of thick and 3.14×10^{-4} m^2 in cross section, when Young's Moduli of the samples were 0.30, 0.75, and 1.42 MPa, respectively. Thrusting forces varied from 0.2 N to 2.0 N by 0.2 N. Fig. 4 shows an example of the observed relationships between spring constants of the samples, the normal forces, and the outputs from a strain gauge. Measurement of each condition was conducted just once because repeatability was high. Fig. 4 shows that the gauge outputs increase as the normal force and spring constants increase. Since the tactile sensor has four strain gauges, the mapping table is constructed for each strain gauge. The table is represented as $\hat{K}_i = \theta_i(v_i, F_n)$, where v_i and F_n are the output voltage of the i-th strain gauge and the normal force, respectively. θ_i linearly interpolates the points in the table, as shown in Fig. 4. For example, when v_i and F_n are measured by the tactile sensor, three neighborhood points are found in the table. A plane $g(\hat{K}, v, F) = 0$ is formed by these three points. By solving $g(\hat{K}_i, v_i, F_n) = 0$, $\hat{K}_i$ is estimated. The final value of the estimated spring constant is determined by the average value from the four mapping tables.

In order to validate this estimation method, we carried out an experiment in which the sensor was moved in the normal direction and thrust into the softness specimen made from silicone rubber. No lateral movement was applied to the sensor. Fig. 5 shows the average and standard deviation of the estimated spring constant when $F_n = 1.0$ and 1.5 N. The maximum error of the estimation was 44%. This error comes from a sparse setting of the spring constants of the rubber samples for the mapping model. More gradual sampling of the spring constants will improve the accuracy of the estimation. The estimation is affected by the surface shape of the contact area, which is considered a natural behavior because human-perceived softness is also affected by the contact area [22].

For remote transmission, when a lateral force is applied to the tactile sensor, this estimation method is not available because the estimation table was constructed from the data acquired with no applied lateral force. Therefore, the estimation of the spring constant was performed only when $|F_t| < 0.3$ N. When the estimation does not work, the adjacent estimated value is used as a current spring constant. In this condition, the slave arm usually estimates the spring constant only at the initial contact with the object. This can be a limitation, but the estimation is done relatively rapidly and robustly. The update rate of the estimation was 125 Hz.

V. Tactile Display Methods

A. Roughness Property

As described in Section II-B, a tactile-displaying method and local model for the roughness property are basically the same as a previously reported method [14]. The previous method has successfully transmitted the roughness sensations of grating scales with surface wavelengths varying from 0.8 mm to 2.0 mm by 0.2 mm. In this study, we extended the previous method for multiple wavelengths of texture surface. When the surface wavelengths consist of λ_1, λ_2, ...λ_N, deformations of the finger skin in stroking the texture is approximated as

$$y(t) = \sum_{i=1}^{N} A_i \sin\left(2\pi \frac{x(t)}{\lambda_i}\right), \tag{3}$$

where $x(t)$, A_i, and N are the finger position on the texture, amplitude of skin deformation caused by the component of λ_i, and the number of surface wavelengths the texture has, respectively. λ_i and A_i are determined from FFT from the outputs of the tactile sensor, which is described in Section V-A. N affects the quality of the roughness stimuli transmitted to the operator. In this study, N was set to 3 because our preliminary evaluation showed little difference in the quality of roughness when N is larger than 3. The electric voltage applied to the tactile stimulator is given by

$$y_r(t) = \alpha y(t), \tag{4}$$

where α [V] is a scaling constant to transform the roughness stimuli to the voltage.

B. Friction Property

As described in Section II-C, the local model and tactile-displaying method for the friction property are based on our previous study [12]. In this study, we made several improvements on the waveforms. Fig. 6 shows the concept of the display method. The method represents the friction sensation of the stick-slip transition by controlling the FA II activities using high-frequency vibration, which is just sensitive to FA II. As shown in Fig. 6, at the transition from

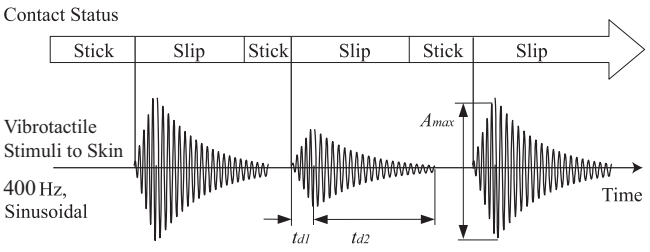

Fig. 6. Concept of Displaying Method for Friction Sensation (modified from [12])

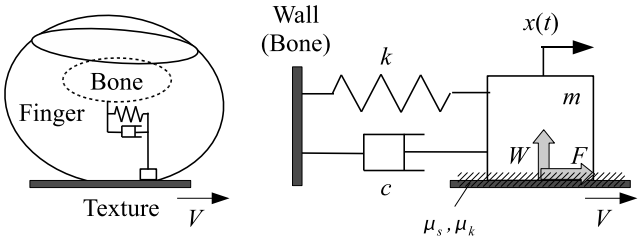

Fig. 7. Single-DOF Vibration Model for Simulating Stick-Slip Motion

the sticking phase to the slipping phase, FA II is stimulated by a burst-like waveform vibration at the frequency of 400 Hz, at which frequency FA II is more sensitive than the other mechanoreceptors. In our previous study [12], the envelope of the waveform had a step-wise shape. This caused an unnatural feeling, similar to a flicking action. In this study, we increased the amplitude of the vibration gradually (t_{d1} period). After the peak, the envelope decayed gradually based on the viscosity of the skin (t_{d2} period). The peak amplitude A_{max} depends on the elastic energy that is stored during the sticking phase.

Fig. 7 illustrates the single-DOF vibration model with a Coulomb friction to generate the approximated stick-slip transition at the finger skin, as described in Section II-C. The mass in the model is coupled with the wall (Bone). This model assumes the texture moves and the wall is connected to the ground. $x(t)$, V, and W are the displacement between the mass and wall, the moving velocity of the texture, and the normal force applied to the skin, respectively. μ_s and μ_k are the static and kinetic friction coefficients, respectively. F is the lateral force applied to the skin, which depends on the contact status of the skin. When the skin is in the sticking phase ($\dot{x}(t) = V$), F is equal to the static friction force. When the force exerted to the mass exceeds the maximum static friction force, the contact status changes from the sticking to slipping phase. This condition is described as

$$m\ddot{x} + c\dot{x} + k(x - x_0) > \mu_s W, \tag{5}$$

Where x_0 is the equilibrium position of the spring.

After the mass starts slipping, it vibrates if the system is not over damping. In the slipping phase, F is equal to the kinetic friction force. Therefore, the equation of motion is given by

$$m\ddot{x} + c\dot{x} + k(x - x_0) + sgn(\dot{x} - V)\mu_k W = 0, \tag{6}$$

where μ_k is kinetic friction coefficient. When the velocity of the mass $\dot{x}(t)$ becomes equal to V, the contact status changes to be the sticking phase again. $\dot{x}(t)$ in the slipping phase is analytically given by solving (6) [12].

As mentioned in II-C, the physical parameters in the model are substituted by the fixed parameter, which was determined by the observation (using a high-speed camera and force sensors) of the stick-slip phenomena of the human finger skin in contact with an acrylic plate [12]. m, c, and k were 1×10^{-6} kg, 1×10^{-5} Ns/m, and 2 N/m, respectively.

The electric voltage applied to the tactile stimulator at the stick-to-slip transition is

$$y_f(t) = A_f \sin(2\pi f_1 t), \tag{7}$$

where A_f is the amplitude of the vibratory stimuli and f_1 is the vibration frequency (400 Hz). A_f is determined by

$$A_f = \begin{cases} \dfrac{A_{max}}{t_{d1}}(t - t_s) & \text{if } (t - t_s) < t_{d1} \\ \dfrac{A_{max}}{t_{d2}^2}(t - t_s - t_{d2})^2 & \text{if } t_{d1} < (t - t_s) < t_{d2}, \end{cases} \tag{8}$$

where A_{max} and t_s are the maximum amplitude of vibratory stimuli, and the time at which the stick-to-slip transition occurred, respectively. t_{d1} and t_{d2} are constant values to determine the decay-period of the stimuli. They were set to 5 and 30 ms in our preliminary adjustments. These parameters should be optimized in the future. A_{max} is defined to be proportional to the restoring force of the spring. A_{max} is given by

$$A_{max} = \beta k(x - x_0), \tag{9}$$

where β [V/N] is a scaling constant to transform the vibratory stimuli to the voltage applied to the stimulator.

C. Softness Property

As described in Section II-C, a tactile display method for the softness property is based on stimulation of SA I, assuming that SA I is related to the perception of the contact area, which corresponds to human-perceived softness [22]. This method controls the activity of SA I using the amplitude of vibrotactile stimuli, which is low-frequency ($<$ 5 Hz). When the spring constant of the object becomes small, the contact area of the finger skin increases and the population of the activated SA I is also expected to increase. In this study, we assumed that the relationship between the spring constant and the amount of SA I stimulation is inversely proportional. The actual relationship should be determined in the future.

The vibrotactile stimuli for softness sensations $y_s(t)$ is determined by,

$$y_s(t) = \frac{\gamma}{K} \sin(2\pi f_2 t), \tag{10}$$

where K is the spring constant of the object. f_2 is the vibration frequency ($f_2 = 5$ Hz), and γ [$10^4\times$ V N/m] is a scaling constant to transform the vibrotactile stimuli to the voltage applied to the stimulating actuator.

D. Integration of All Properties

For integrating all the tactile properties, the superposition of eqs. (4), (7), and (10) is applied for the electric voltage $V(t)$ to the voice coil as follows:

$$V(t) = y_r(t) + y_f(t) + y_s(t), \tag{11}$$

where $y_r(t)$, $y_f(t)$, and $y_s(t)$, are the displayed signals for roughness, friction, and soft properties, respectively.

The magnitude of each perceived property is adjusted by the scaling constants, which are α, β, and γ in eqs. (4), (7), and (10), respectively. In order to present a natural feeling to the operator, we should select the optimal scaling constants. In this study, however, the scaling factors were determined by an expert who is an author of this paper and has good tactile sensitivity because the purpose of this study was to confirm the feasibility of a combination of selected multiple tactile properties. As a result, we determined that $\alpha = 0.4$, $\beta = 3.5$, and $\gamma = 2.0$.

TABLE I

ANSWER RATINGS OF MATERIAL DISCRIMINATION EXPERIMENT

		Answer				
		Embossed Paper	Grating Scale	Copying Paper	Fleece Fabric	Boa Fabric
Displayed Material	Embossed Paper (unevenly rough and hard)	0.90 ± 0.10 (0.23 ± 0.06)	0.10 ± 0.10 (0.10 ± 0.10)	0.00 ± 0.00 (0.53 ± 0.15)	0.00 ± 0.00 (0.10 ± 0.00)	0.00 ± 0.00 (0.03 ± 0.06)
	Grating Scale (uniformly rough and hard)	0.13 ± 0.23 (0.23 ± 0.12)	0.73 ± 0.15 (0.27 ± 0.15)	0.07 ± 0.06 (0.17 ± 0.06)	0.03 ± 0.06 (0.27 ± 0.15)	0.03 ± 0.06 (0.07 ± 0.06)
	Copying Paper (flat and hard)	0.00 ± 0.00 (0.21 ± 0.10)	0.00 ± 0.00 (0.03 ± 0.06)	0.57 ± 0.21 (0.31 ± 0.12)	0.27 ± 0.21 (0.41 ± 0.20)	0.17 ± 0.21 (0.03 ± 0.06)
	Fleece Fabric (smooth and soft)	0.00 ± 0.00 (0.10 ± 0.00)	0.00 ± 0.00 (0.13 ± 0.06)	0.20 ± 0.10 (0.17 ± 0.21)	0.70 ± 0.10 (0.43 ± 0.21)	0.10 ± 0.10 (0.17 ± 0.06)
	Boa Fabric (rough and soft)	0.00 ± 0.00 (0.17 ± 0.06)	0.03 ± 0.06 (0.03 ± 0.06)	0.07 ± 0.06 (0.07 ± 0.12)	0.20 ± 0.10 (0.17 ± 0.06)	0.70 ± 0.17 (0.57 ± 0.15)

Values in parentheses are the answer ratings for the master-slave system with force feedback only. Gray cells indicate correct answer ratings.

VI. EXPERIMENT: MATERIAL DISCRIMINATION

An experiment in which the participants explored and discerned materials through the developed master-slave system was performed. It is important to evaluate the transmission of each tactile property thoroughly. However, before we conduct the detailed experiments and analysis, we needed to confirm the total potential for our selection of tactile properties through a feasibility study. This study evaluated the total performance for material discrimination involving all three tactile properties. As a reference, we also compared our results with the performance from force feedback without tactile feedbacks.

A. Experimental Procedures

Using the tactile transmission system developed as described in Section III, an experiment to discriminate five types of materials was conducted. The experiment was performed under two different feedback conditions. Under the first condition, both the tactile feedback and force feedback were available, while in the second condition, only the force feedback was available.

The participants explored five types of materials through the developed master-slave system. Five materials were an embossed coated paper (unevenly rough and hard), an acrylic grating scale with a surface wavelength of 1.5 mm (uniformly rough and hard), a piece of copy paper (flat and hard), a fleece fabric approximately 3 mm thick (smooth and soft), and a boa fabric approximately 7 mm thick (rough and soft).

The participants were instructed to identify the material that they felt was closest to the one they explored through the master-slave system. The participants were not allowed to see the slave side and heard a pink noise over the headphones. As comparison stimuli, the same materials were prepared in order for the participants to freely explore the materials with their bare fingers during the experiment.

For each material, 10 trials were performed. In total, each participant performed 50 trials. After the first 25 trials, the participants took a 5-minute break. No time limit was set for the trials. The material was displayed in a random order. The participants practiced before the main trials for approximately 3 minutes. The number of participants was three. All the participants were studying haptic research and had previous experience in using tactile displays.

B. Experimental Results

Table I lists the average answer ratings and the standard deviation of the experiment for each material. Gray cells indicate the correct answer ratings. Values in parentheses are the ratings for the force feedback only system.

The correct answer ratings with the tactile feedback system show good potential over 70% except for the paper (57%). From the results, we confirmed the feasibility of the total performance of the integrated multiple tactile properties. The correct answer ratings, however, depended on the materials. Optimization of each tactile display and of the sensing methods is required. In addition, there is a possibility that the three tactile properties selected are not sufficient for transmitting total touch feelings. Further investigation is needed in the future.

The correct answer ratings for the tactile feedback system tend to be higher than those for the force feedback system. In particular, in the force feedback condition, the correct answer ratings for the embossed paper and grating scale were approximately at chance level, while in the tactile feedback condition, the correct answer ratings for these materials were much higher. A two-way ANOVA was applied to the correct answer ratings, with the factors being a type of feedback and a type of material. The test showed that there was a significant difference in the correct answer ratings between the force feedback and the tactile feedback systems ($F(1, 20) = 40.5$, $p = 3.29 \times 10^{-6}$), with no significant interaction between the two factors.

VII. CONCLUSIONS

In this study, we developed a tactile transmission system that transmits multiple tactile properties of roughness, softness, and friction sensations from remote environments. We report the first trial of the integration of our tactile display methods and sensing methods for multiple tactile properties. We discussed the system design from the viewpoint of selection of multiple tactile properties, synchronization of hand exploration and tactile feedback, and transmission method between measured and displayed signals. In order to compensate for communication time delay for the three tactile properties, local models and display methods that involved physical parameters and explored the movements of operators were constructed. We also enhanced the tactile sensing methods proposed in our previous studies to achieve more detail in real time.

Fig. 8. World's First Demonstration of Remote Tactile Transmission between Tokyo and Sendai

To confirm the feasibility of the total system involving the three selected tactile properties, we performed an experiment pertaining to material discrimination. The results showed the potential for discrimination to be mostly over 70% of the correct answer ratings. The detailed evaluation and analysis of the potential of individual tactile properties will be reported in our next paper.

We demonstrated the performance of the tactile transmission system in an actual remote environment at the 14th Annual Conference of the Virtual Reality Society of Japan (September 9–11, 2009, Waseda University). Fig. 8 shows a photograph of the demonstration. We were able to deliver multiple tactile properties from Tohoku University in Sendai to the operators at Waseda University in Tokyo; the direct distance between these two locations is 300 km. As for the communication delay, the round-trip time of the PING command was 20 – 25 ms, which was relatively stable. Many operators, who were participants at the conference, could discriminate between the touch of different materials (fleece, embossed paper, fake leather, etc.) placed at the remote site. To our knowledge, this demonstration is one of the world's first remote tactile transmission that includes multiple tactile properties.

ACKNOWLEDGEMENTS

This study was partially supported by a Grant-in-Aid for Scientific Research B (18760179) and a grant from the Ministry of Internal Affairs and Communications SCOPE (082102006).

REFERENCES

[1] S. Okamoto, M. Konyo, S. Saga, and S. Tadokoro, "Detectability and Perceptual Consequences of Delayed Feedback in a Vibrotactile Texture Display," *IEEE Trans. on Haptics,* vol. 2, issue 2, pp. 73-84, 2009.

[2] R. D. Howe, W. J. Peine, D. A. Kontarinis and J. S. Son, "Remote Palpation Technology," *IEEE Eng. in Medicine and Biology,* vol. 14, no. 3, pp. 318–323, 1995.

[3] M. V. Ottermo, "Virtual Palpation Gripper," *Ph.D. Thesis of Norwegian University of Science & Technology* 2006

[4] F. E. Fan, M. O. Culjat, C. King, M. L. Franco, R. Boryk, J. W. Bisley, "A Haptic Feedback System for Lower-limb Prostheses," *IEEE Trans. Neural Systems and Rehabilitation Eng.,* vol. 16, no. 3, pp. 270–277, 2008.

[5] K. Warwick, M. Gasson, B. Hutt, I. Goodhew, P. Kyberd, B. Andrews, P. Teddy and A. Shad, "The Application of Implant Technology for Cybernetic Systems," *Archives of Neurology,* vol. 60, no. 10, pp. 1369–1373, 2003

[6] M. Shimojo, T. Suzuki, A. Namiki, T. Saito, M. Kunimoto, R. Makino, H. Ogawa and M. Ishikawa, "Development of a System for Experiencing Tactile Sensation from a Robot Hand by Electrically Stimulating Sensory Nerve Fiber," *Proc. of the 2003 IEEE Int'l Conf. on Robotics & Automation,* pp. 1264–1270, 2003

[7] D. A. Kontarinis and R. D. Howe, "Tactile Display of Vibratory Information in Teleoperation and Virtual Environments," *Presence,* vol. 4, no. 4, pp. 387–402, 1995

[8] J. T. Dennerlein, P. A. Millman and R. D. Howe, "Vibrotactile Feedback for Industrial Telemanipulators," *Proc. of the Sixth Annual Symposium on Haptic Interfaces for Virtual Environment and Teleoperator Systems, ASME Int'l Mechanical Engineering Congress & Exposition,* pp. 189–195, 1997

[9] A. Yamamoto, S. Nagasawa, H. Yamamoto and T. Higuchi, "Electrostatic Tactile Display with Thin Film Slider and its Application to Tactile Telepresentation System," *IEEE Trans. on Visualization and Computer Graphics,* vol. 12, no. 2, pp. 168–177, 2006

[10] D. G. Caldwell, and C. Gosney, "Enhanced Tactile Feedback (Tele-Taction) using a Multi-Functional Sensory System," *Proc. of the 1993 IEEE Int'l Conf. on Robotics and Automation,* pp. 955–960, 1993

[11] M. Konyo, S. Tadokoro, A. Yoshida, and N. Saiwaki, "A Tactile Synthesis Method Using Multiple Frequency Vibrations for Representing Virtual Touch," *Proc. of the 2005 IEEE/RSJ Int'l Conf. on Intelligent Robots and Systems,* pp. 3965–3971, 2005.

[12] M. Konyo, H. Yamada, S. Okamoto, and S. Tadokoro, "Alternative Display of Friction Represented by Tactile Stimulation without Tangential Force," *Haptics: Perception, Devices and Scenarios, Lecture Notes in Computer Science,* vol. 5024, pp. 619–629, Heidelberg, Germany: Springer, 2008.

[13] Y. Mukaibo, H. Shirado, M. Konyo, and T. Maeno, "Development of a Texture Sensor Emulating the Tissue Structure and Perceptual Mechanism of Human Fingers," *Proc. of the 2005 IEEE Int'l Conf. on Robotics and Automation,* pp. 2565–2570, 2005.

[14] S. Okamoto, M. Konyo, T. Maeno, and S. Tadokoro, "Transmission of Tactile Roughness through Master-slave Systems," *Proc. of the 2009 IEEE Int'l Conf. on Robotics and Automation,* pp. 1467–1472, 2009.

[15] A. K. Bejczy, W. S. Kim, and S. C. Venema, "The Phantom Robot: Predictive Displays for Teleoperation with Time Delay," *Proc. of the 1990 IEEE Int'l Conf. on Robotics and Automation,* pp. 546–551, 1990.

[16] T. Kotoku, "A Predictive Display with Force Feedback and its Application to Remote Manipulation System with Transmission Time Delay," *Proc. of the 1992 IEEE/RSJ Int'l Conf. on Intelligent Robots and Systems,* pp. 239–246, 1992.

[17] L. A. Jones, and S. J. Lederman, "Human Hand Function", Oxford, UK: Oxford University Press, 2006.

[18] M. Hollins, S. Bensmaia, K. Karlof, and F. Young, "Individual Differences in Perceptual Space for Tactile Textures: Evidence from Multidimensional Scaling," *Perception & Psychophysics,* vol. 62, pp. 1534–1544, 2000.

[19] T. Yoshioka, S. J. Bensmaia, J. C. Craig, and S. S. Hsiao, "Texture perception through direct and indirect touch: An analysis of perceptual space for tactile textures in two modes of exploration," *Somatosensory and Motor Research,* vol. 24, pp. 53–70, 2007.

[20] H. Shirado, Y. Nonomura, and T. Maeno, "Realization of Human Skin-like Texture by Emulating Surface Shape Pattern and Elastic Structure" *Proc. of the 2006 IEEE Symposium on Haptic Interfaces for Virtual Environment and Teleoperator Systems,* pp. 295–296, 2006.

[21] Y. Nonomura, T. Fujii, Y. Arashi, T. Miura, T. Maeno, K. Tashiro, Y. Kamikawa, and R. Monchi, "Tactile Impression and Friction of Water on Human Skin," *Colloids and Surfaces B: Biointerfaces,* vol. 69, pp. 264–267, 2009.

[22] A. Bicchi, E. P. Scilingo, D. De Rossi, "Haptic Discrimination of Softness in Teleoperation: The Role of the Contact Area Spread Rate," *IEEE Trans. Robotics & Automation,* vol. 16, no. 5, pp. 496–504, 2000.

[23] Y. Hidaka, Y. Shiokawa, K. Tashiro, T. Maeno, M. Konyo and T. Yamauchi, "Development of an Elastic Tactile Sensor Emulating Human Fingers for Tele-Presentation Systems," *Proc. of the IEEE SENSORS 2009 Conf.,* pp.1919–1922, 2009.